



**HAL**  
open science

## Pairing Forces Govern Population of Doubly Magic $^{54}\text{Ca}$ from Direct Reactions

F. Browne, S. Chen, P. Doornenbal, A. Obertelli, K. Ogata, Y. Utsuno, K.  
Yoshida, N.L. Achouri, H. Baba, D. Calvet, et al.

► **To cite this version:**

F. Browne, S. Chen, P. Doornenbal, A. Obertelli, K. Ogata, et al.. Pairing Forces Govern Population of Doubly Magic  $^{54}\text{Ca}$  from Direct Reactions. *Phys.Rev.Lett.*, 2021, 126 (25), pp.252501. 10.1103/PhysRevLett.126.252501 . hal-03273401

**HAL Id: hal-03273401**

**<https://hal.science/hal-03273401>**

Submitted on 12 Jul 2021

**HAL** is a multi-disciplinary open access archive for the deposit and dissemination of scientific research documents, whether they are published or not. The documents may come from teaching and research institutions in France or abroad, or from public or private research centers.

L'archive ouverte pluridisciplinaire **HAL**, est destinée au dépôt et à la diffusion de documents scientifiques de niveau recherche, publiés ou non, émanant des établissements d'enseignement et de recherche français ou étrangers, des laboratoires publics ou privés.

# Pairing forces govern population of doubly magic $^{54}\text{Ca}$ from direct reactions

F. Browne,<sup>1,\*</sup> S. Chen,<sup>2,1,3</sup> P. Doornenbal,<sup>1</sup> A. Obertelli,<sup>4,5,1</sup> K. Ogata,<sup>6,7</sup> Y. Utsuno,<sup>8,9</sup> K. Yoshida,<sup>9</sup> N. L. Achouri,<sup>10</sup> H. Baba,<sup>1</sup> D. Calvet,<sup>5</sup> F. Château,<sup>5</sup> N. Chiga,<sup>1</sup> A. Corsi,<sup>5</sup> M. L. Cortés,<sup>1</sup> A. Delbart,<sup>5</sup> J.-M. Gheller,<sup>5</sup> A. Giganon,<sup>5</sup> A. Gillibert,<sup>5</sup> C. Hilaire,<sup>5</sup> T. Isobe,<sup>1</sup> T. Kobayashi,<sup>11</sup> Y. Kubota,<sup>1,8</sup> V. Lapoux,<sup>5</sup> H. N. Liu,<sup>5,12</sup> T. Motobayashi,<sup>1</sup> I. Murray,<sup>13,1</sup> H. Otsu,<sup>1</sup> V. Panin,<sup>1</sup> N. Paul,<sup>5</sup> W. Rodriguez,<sup>14,1,15</sup> H. Sakurai,<sup>1,16</sup> M. Sasano,<sup>1</sup> D. Steppenbeck,<sup>1</sup> L. Stuhl,<sup>8</sup> Y. L. Sun,<sup>5</sup> Y. Togano,<sup>17</sup> T. Uesaka,<sup>1</sup> K. Wimmer,<sup>16,1,†</sup> K. Yoneda,<sup>1</sup> O. Aktas,<sup>12</sup> T. Aumann,<sup>4,18</sup> L. X. Chung,<sup>19</sup> F. Flavigny,<sup>13</sup> S. Franchoo,<sup>13</sup> I. Gasparic,<sup>20,1</sup> R.-B. Gerst,<sup>21</sup> J. Gibelin,<sup>10</sup> K. I. Hahn,<sup>22</sup> D. Kim,<sup>22</sup> T. Koiwai,<sup>16</sup> Y. Kondo,<sup>23</sup> P. Koseoglou,<sup>4,18</sup> J. Lee,<sup>2</sup> C. Lehr,<sup>4</sup> B. D. Linh,<sup>19</sup> T. Lokotko,<sup>2</sup> M. MacCormick,<sup>13</sup> K. Moschner,<sup>21</sup> T. Nakamura,<sup>23</sup> S. Y. Park,<sup>22</sup> D. Rossi,<sup>4,18</sup> E. Sahin,<sup>24</sup> P.-A. Söderström,<sup>4</sup> D. Sohler,<sup>25</sup> S. Takeuchi,<sup>23</sup> H. Toernqvist,<sup>4,18</sup> V. Vaquero,<sup>26</sup> V. Wagner,<sup>4</sup> S. Wang,<sup>27</sup> V. Werner,<sup>4</sup> X. Xu,<sup>2</sup> H. Yamada,<sup>23</sup> D. Yan,<sup>27</sup> Z. Yang,<sup>1</sup> M. Yasuda,<sup>23</sup> and L. Zanetti<sup>4</sup>

<sup>1</sup>RIKEN Nishina Center, 2-1 Hirosawa, Wako, Saitama 351-0198, Japan

<sup>2</sup>Department of Physics, The University of Hong Kong, Pokfulam, 999077, Hong Kong

<sup>3</sup>State Key Laboratory of Nuclear Physics and Technology, Peking University, Beijing 100871, P.R. China

<sup>4</sup>Institut für Kernphysik, Technische Universität Darmstadt, 64289 Darmstadt, Germany

<sup>5</sup>IRFU, CEA, Université Paris-Saclay, F-91191 Gif-sur-Yvette, France

<sup>6</sup>Research Center for Nuclear Physics (RCNP), Osaka University, Ibaraki 567-0047, Japan

<sup>7</sup>Department of Physics, Osaka City University, Osaka 558-8585, Japan

<sup>8</sup>Center for Nuclear Study, University of Tokyo, RIKEN campus, Wako, Saitama 351-0198, Japan

<sup>9</sup>Advanced Science Research Center, Japan Atomic Energy Agency, Tokai, Ibaraki 319-1195, Japan

<sup>10</sup>LPC Caen, ENSICAEN, Université de Caen, CNRS/IN2P3, F-14050 Caen, France

<sup>11</sup>Department of Physics, Tohoku University, Sendai 980-8578, Japan

<sup>12</sup>KTH Royal Institute of Technology, 10691 Stockholm, Sweden

<sup>13</sup>IPN Orsay, CNRS and Université Paris-Saclay, F-91406 Orsay Cedex, France

<sup>14</sup>Universidad Nacional de Colombia, Carr. 30 No. 45-03, Bogotá, Colombia

<sup>15</sup>Pontificia Universidad Javeriana, Facultad de Ciencias, Departamento de Física, Bogotá, Colombia

<sup>16</sup>Department of Physics, University of Tokyo, 7-3-1 Hongo, Bunkyo, Tokyo 113-0033, Japan

<sup>17</sup>Department of Physics, Rikkyo University, 3-34-1 Nishi-Ikebukuro, Toshima, Tokyo 171-8501, Japan

<sup>18</sup>GSI Helmholtzzentrum für Schwerionenforschung GmbH, Planckstr. 1, 64291 Darmstadt, Germany

<sup>19</sup>Institute for Nuclear Science & Technology, VINATOM, 179 Hoang Quoc Viet, Cau Giay, Hanoi, Vietnam

<sup>20</sup>Ruder Bošković Institute, Bijenička cesta 54, 10000 Zagreb, Croatia

<sup>21</sup>Institut für Kernphysik, Universität zu Köln, D-50937 Cologne, Germany

<sup>22</sup>Ewha Womans University, Seoul, South Korea

<sup>23</sup>Department of Physics, Tokyo Institute of Technology, 2-12-1 O-Okayama, Meguro, Tokyo, 152-8551, Japan

<sup>24</sup>Department of Physics, University of Oslo, N-0316 Oslo, Norway

<sup>25</sup>Atomki, P.O. Box 51, Debrecen H-4001, Hungary

<sup>26</sup>Instituto de Estructura de la Materia, CSIC, E-28006 Madrid, Spain

<sup>27</sup>Institute of Modern Physics, Chinese Academy of Sciences, Lanzhou, China

(Dated: January 11, 2021)

Direct proton-knockout reactions of  $^{55}\text{Sc}$  at  $\sim 200$  MeV/nucleon were studied at the RIKEN Radioactive Isotope Beam Factory. Populated states of  $^{54}\text{Ca}$  were investigated through  $\gamma$ -ray and invariant-mass spectroscopy. State energies were calculated from the shell model, employing the GXPF1Br interaction, and their exclusive cross sections from distorted-wave impulse approximation single-particle estimates factored with the shell model spectroscopic factors. Despite the calculations showing a significant amplitude of excited neutron configurations in the ground-state of  $^{55}\text{Sc}$ , valence proton removals populated predominantly the ground-state of  $^{54}\text{Ca}$ . This counter-intuitive result is attributed to pairing effects leading to a dominance of the ground-state spectroscopic factor. Owing to the ubiquity of the pairing interaction, this argument should be generally applicable to direct knockout reactions from odd-even to even-even nuclei.

Perhaps the most profound of the interactions within the atomic nucleus is that of *pairing*. It is well described by a strongly attractive contact force between two nucleons (protons and neutrons). Notably, it is why, without exception, even-even nuclei have zero total angular momentum and positive parity,  $J^\pi = 0^+$ , ground states. Moreover, it is the origin of odd-even staggering of neutron and proton separation energies ( $S_n$  and  $S_p$ , respectively). Recently, pairing has been shown to have a prominent role in single-nucleon removal cross sections in so-called *neutron-rich exotic nuclei* which have an excess of neutrons compared to their stable counterparts [1]. In this Letter, a further implication of pairing to direct reactions is demonstrated.

64 Along with pairing, the interaction of a nucleon's intrinsic ( $s$ ) and orbital ( $\ell$ ) angular momenta has far-  
 65 reaching consequences. In particular, it is necessary  
 66 for the theoretical reproduction of the canonical nuclear  
 67 "magic numbers" [2, 3], 2, 8, 20, 28, 50, 82..., which re-  
 68 late to large energy gaps between shells of protons and  
 69 neutrons. Nuclei with both proton and neutron numbers  
 70 equalling magic numbers are known as *doubly magic*. A  
 71 consequence of the pairing interaction, most obvious in  
 72 doubly magic nuclei, is the existence of excited states  
 73 doubly magic nuclei, is the existence of excited states  
 74 based on the promotion of identical nucleon pairs to  
 75 higher-lying shells into 2-particle-2-hole (2p-2h) states.

76 A feature of the *tensor force*, which describes meson  
 77 exchanges between nucleons, is the attraction of unlike  
 78 nucleons of the same  $\ell$  ( $= s, p, d, f, \dots$ ) with different in-  
 79 trinsic spin directions,  $j_> = \ell + s$  and  $j_< = \ell - s$ ,  
 80 where  $E(j_>) < E(j_<)$  [4]. It implies an evolution of  
 81 the energies of the spin-orbit generated shells as a func-  
 82 tion of nucleon number in exotic nuclei [5, 6]. Stable  
 83 counterparts of neutron-rich nuclei have occupied proton  
 84  $j_>$  orbits, lowering the corresponding neutron  $j_<$  or-  
 85 bital energy. Low occupancy of the proton  $j_>$  in the  
 86 neutron-rich case results in less interaction with the neu-  
 87 tron  $j_<$  orbital allowing  $E(j_<)$  to increase. In  $^{54}\text{Ca}$ , this  
 88 effect, owing to a lack of  $\pi(\text{proton})0f_{7/2}$  occupation, al-  
 89 lows for a high-lying  $\nu(\text{neutron})0f_{5/2}$  orbital which cre-  
 90 ates the non-canonical  $N(\text{neutron number}) = 34$  magic  
 91 number [7–9]. A direct analogue exists in  $^{24}\text{O}$  where an  
 92 unoccupied  $\pi 0d_{5/2}$  orbital allows a large, compared even  
 93 to the nearby  $^{27}\text{Ne}$  [10], gap between  $\nu 0d_{3/2}$  and  $\nu 1s_{1/2}$ ,  
 94 to form, leading to the non-canonical  $N = 16$  magic num-  
 95 ber [11, 12].

96 There is some recent evidence that the removal of the  
 97 valence proton from the  $\pi 0d_{5/2}$  orbital in  $^{25}\text{F}$  leads to  
 98  $\sim 60\%$  population of excited states of  $^{24}\text{O}$  [13]. The ex-  
 99 planation for this in Ref. [13] was the induced configura-  
 100 tion mixing of the  $^{24}\text{O}$  core neutron states by the lowering  
 101 of the  $\nu 0d_{3/2}$  energy through an artificially strengthened  
 102 tensor interaction with the  $\pi 0d_{5/2}$  proton. However, from  
 103 the point of view of the pairing interaction, the spectro-  
 104 scopic factor to the ground-state would be expected to be  
 105 large. This can be illustrated in a two-level model of  
 106  $0p-0h$  (ground state) and  $2p-2h$  neutron states for  $^{25}\text{F}$   
 107 and  $^{24}\text{O}$ . The spectroscopic factor to the ground-state  
 108 of  $^{24}\text{O}$  following a  $\pi 0d_{3/2}$  proton removal is dependent  
 109 on the product of amplitudes of the  $2p-2h$  states in  $^{25}\text{F}$   
 110 and  $^{24}\text{O}$  which is positive owing to the definite signs of  
 111 the off-diagonal two-body matrix elements of the pairing  
 112 interaction [14].

113 Whether the population patterns from direct proton  
 114 removal reactions  $^{55}\text{Sc}(p, 2p)$  adhere to the pairing inter-  
 115 action expectation or tensor-driven effects is addressed in  
 116 this letter. As with  $^{25}\text{F}$ ,  $^{55}\text{Sc}$  has a non-canonical doubly  
 117 magic core that results from the absence of tensor-driven  
 118 attraction and a single proton in the orbital that acts to  
 119 lower the valence neutron energies. In the present work

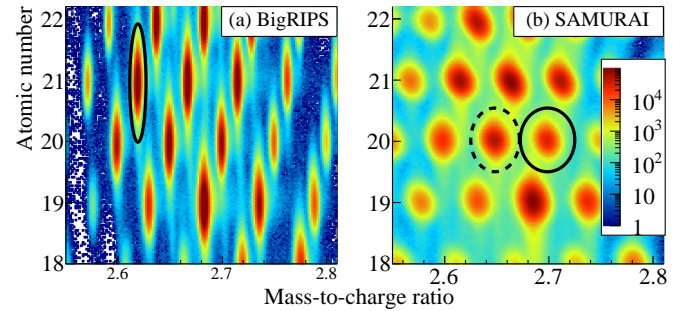


FIG. 1. Identified ions in front of (a) and behind (b) the reaction target. In (a), the ellipse indicates the software gate placed on  $^{55}\text{Sc}$ . In (b), gates applied to select  $^{53}\text{Ca}$  and  $^{54}\text{Ca}$  are shown as dashed and solid ellipses, respectively. The scale is counts per bin and applies to (a) and (b).

120 and Ref. [13], projectiles were produced under the same  
 121 conditions and the same reaction is employed at an en-  
 122 ergy of  $\sim 200$  MeV/nucleon.

123 The first study of  $^{54}\text{Ca}$  populated through direct re-  
 124 actions is presented. Exclusive cross sections of ground  
 125 and excited states have been measured as well as  $\ell$  values  
 126 of removed nucleons that populated them. Only through  
 127 application of invariant-mass spectroscopy to the heav-  
 128 ily exotic nucleus to date were such measurements pos-  
 129 sible for the unbound states. Comparisons of the mea-  
 130 surements were made to distorted-wave impulse approx-  
 131 imation (DWIA) [15, 16] and conventional shell model  
 132 calculations, the latter employing the GXPF1Br inter-  
 133 action [7] in the full  $sd$ - $pf$ - $gds$  model space. From the com-  
 134 parisons,  $\ell$  values of removed nucleons and tentative  $J^\pi$   
 135 assignments to excited states of  $^{54}\text{Ca}$  were determined.  
 136 The results show predominant ground- and excited-state  
 137 population of  $^{54}\text{Ca}$  through valence and core proton re-  
 138 movals, respectively.

139 Experimental investigations were conducted at the Ra-  
 140 dioactive Isotope Beam Factory, operated by the RIKEN  
 141 Nishina Center and the Center for Nuclear Study, Uni-  
 142 versity of Tokyo. A 240 pA beam of  $^{70}\text{Zn}^{30+}$  was ac-  
 143 celerated to 345 MeV/nucleon and secondary beams of  
 144 isotopes produced from its fragmentation on a 10-mm-  
 145 thick  $^9\text{Be}$  target situated at the entrance of BigRIPS [18],  
 146 a two-stage fragment separator. Constituents of the  
 147 secondary beams were selected and separated up until  
 148 the 3<sup>rd</sup> focal plane of BigRIPS by their magnetic rigid-  
 149 ity ( $B\rho$ ) through two dipole magnets and energy loss  
 150 ( $\Delta E$ ) through an Al wedge-shaped degrader situated be-  
 151 tween the dipole magnets. The time-of-flight (TOF),  
 152  $B\rho$ , and  $\Delta E$  were recorded for each ion between the  
 153 3<sup>rd</sup> and 7<sup>th</sup> focal planes. These measurements were  
 154 combined to provide unambiguous particle identification  
 155 (PID) of the ions' mass-to-charge ratio and atomic num-  
 156 ber [19], shown in Fig. 1(a). Following identification,  
 157 the secondary beams were transported to the MINOS de-  
 158 vice [20], a 151(1)-mm-long liquid hydrogen ( $\text{LH}_2$ ) target

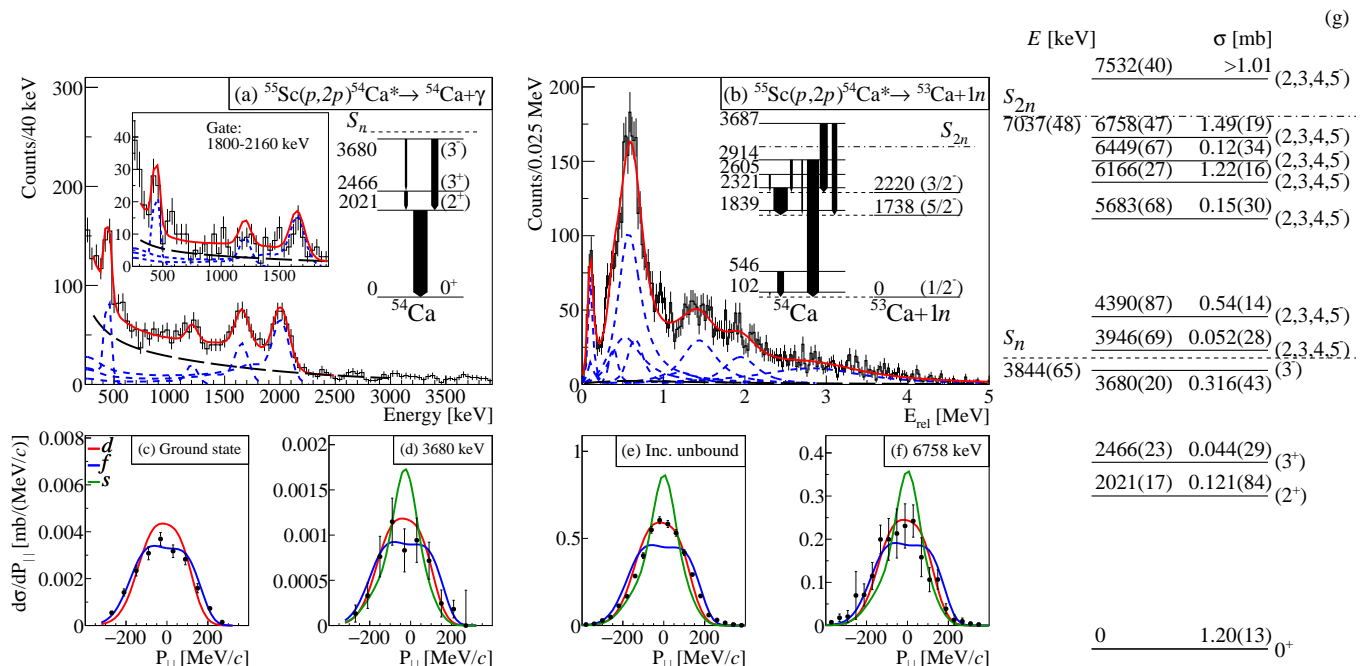


FIG. 2. (a) Doppler-corrected  $\gamma$ -ray spectrum of the  $^{55}\text{Sc}(p,2p)^{54}\text{Ca}^* \rightarrow ^{54}\text{Ca} + \gamma$  reaction populating bound states. The total fit function (red line) comprises simulated response functions of DALI2<sup>+</sup> (blue short-dashed lines) and a double-exponential background (black long-dashed line). The inset spectrum is that in coincidence with the 2021-keV transition, where the blue dashed lines are intensity-fixed responses assuming the shown level scheme. Arrow widths on the level scheme represent relative  $\gamma$ -ray intensities. (b) Relative energy spectrum of  $^{55}\text{Sc}(p,2p)^{54}\text{Ca}^* \rightarrow ^{53}\text{Ca} + 1n$ . The total fit function (red line) is the sum of the simulated responses of NeuLAND+NEBULA and beam-line detectors (blue short-dashed lines), and a non-resonant background (black long-dashed line). Inset is the decay scheme to  $^{53}\text{Ca}$ , level energies are with respect to the  $^{53}\text{Ca}$  ground-state energy and arrow widths are relative decay strengths. (c-f) PMDs of residual  $^{54}\text{Ca}$  (c,d) and  $^{53}\text{Ca} + 1n$  (e,f) following  $^{55}\text{Sc}(p,2p)$  reactions in coincidence with various states. “Inc. unbound” infers the inclusive PMD for unbound states, otherwise labels of (c-f) correspond to (g), which shows the energies, cross sections, and  $J^\pi$  assignments of observed states. Data points in (c-f) are observed and solid curves are predicted by the DWIA for the  $d$ -,  $f$ -, and  $s$ -wave proton removals normalized to experimental cross sections. Where appropriate,  $S_n$  and  $S_{2n}$  [17] values are indicated.

159 surrounded by a time projection chamber (TPC) situ- 180 one assembly of 400  $5 \times 5 \times 250$  cm<sup>3</sup> detectors arranged in  
 160 ated at the focal plane designated “F13” which is  $\sim 40$  m 181 alternating vertically- and horizontally-aligned planes of  
 161 downstream of the 7<sup>th</sup> focal plane. Surrounding MINOS 182 50 detectors. The center of NeuLAND was 11.8 m from  
 162 was the DALI2<sup>+</sup> array of 226 NaI(Tl) crystals [21, 22] 183 the center of the LH<sub>2</sub> target, and the two NEBULA as-  
 163 for the high-efficiency detection ( $\sim 23\%$  for a 2 MeV  $\gamma$  184 ssemblies were at 14.4 and 15.3 m. Neutron energies were  
 164 ray emitted at  $\beta_{\text{ion}} \approx 0.6$ ) of  $\gamma$  rays emitted by ex- 185 calculated from their velocities which were derived from  
 165 cited states populated by secondary reactions. Behind 186 their TOFs and flight paths.  
 166 MINOS, reaction residues were identified, as shown in  
 167 Fig. 1(b), with the SAMURAI spectrometer by their  $B\rho$  187 Doppler-corrected  $\gamma$ -ray spectra following the  
 168 through a single dipole magnet, TOF from the target 188  $^{55}\text{Sc}(p,2p)$  reaction, Fig. 2(a), show  $\gamma$ -ray peaks at  
 169 to a hodoscope, and energy loss in the hodoscope [23]. 189 445(16), 1210(30), 1661(17), and 2021(17) keV, consis-  
 170 Reaction vertices in the LH<sub>2</sub> target were identified with 190 tent with Ref. [7]. Coincidences between the 2021-keV  
 171 a precision of  $\sim 2$  mm ( $\sigma$ ) by tracking incoming frag- 191 transition and all others were observed, shown inset of  
 172 ments with beam-line detectors and tracking protons 192 Fig. 2(a), with intensities which imply the level scheme  
 173 ejected from the target with the surrounding TPC [24]. 193 shown in Fig. 2(a). In the coincidence spectrum, an  
 174 Fragment velocities at the reaction vertex were recon- 194 excess of counts appears at  $\sim 560$  keV, with a corre-  
 175 structed using the vertex position and velocity measured 195 sponding excess in the singles spectrum. Assuming this  
 176 in SAMURAI. Beam-velocity neutron-detection was re- 196 takes the form of a  $\gamma$ -ray transition, a fitted value of  
 177 alised with NEBULA [23, 25], comprising two assem- 197 561(19) keV is obtained with a 0.04(2) mb cross section.  
 178 blies of 60 vertically-aligned  $12 \times 12 \times 180$  cm<sup>3</sup> detectors 198 With a significance of just over  $1\sigma$ , it is not considered  
 179 arranged in a  $2 \times 30$  configuration, and NeuLAND [26], 199 in the calculation of other partial cross sections. The  
 200 strength at  $\sim 300$  keV in the coincidence spectrum is

201 likely Bremsstrahlung background. The parallel momentum distributions (PMDs) of the reaction products in coincidence with their populated state provides information on the  $\ell$ -value of the removed nucleon. PMDs of  $^{54}\text{Ca}$  nuclei in the ground, Fig. 2(c), and  $(3^-)$ , Fig. 2(d), states were measured with a resolution of  $\sim 34$  MeV/c ( $\sigma$ ) which was inferred from unreacted  $^{55}\text{Sc}$  nuclei [27]. The ground-state PMD is inconsistent with the removal of an  $f$ -wave proton and the  $(3^-)$  PMD has  $\chi^2/\text{degree of freedom}$  for the  $d$  and  $f$  curves of 0.56 and 0.64, respectively, slightly favoring the removal from a  $d$  orbital. The  $f$ -like PMD of the ground-state population supports previous evidence for a  $J^\pi = 7/2^-$   $^{55}\text{Sc}$  ground-state [28] it almost certainly reflects a valence  $\pi 0f_{7/2}$  orbital. Since the  $2_1^+$  state population is dominated by feeding from the  $(3^-)$  state, its PMD only reflects the  $(3^-)$  structure, it can be found with the inclusive PMD in Ref. [27]. From these observations and those in Ref. [7], a  $3_1^-$  state with a  $\pi 0f_{7/2}^{-1} 0d_{3/2}^{-1}$  configuration is suggested for the 3680(20) keV level.

221 Decays of unbound states of  $^{54}\text{Ca}$ , first inferred through inelastic scattering [9], are shown in the relative energy ( $E_{\text{rel}}$ ) spectrum of  $^{53}\text{Ca}$  and respective emitted neutrons in Fig. 2(b).  $E_{\text{rel}}$  spectra in coincidence with individual states of  $^{53}\text{Ca}$ , so-called exclusive spectra, were used to isolate overlapping peaks and construct the decay scheme shown in Fig. 2(b) [27]. Peaks were fitted with Breit-Wigner distributions [29] folded with experimental responses of the NeuLAND+NEBULA array and beam-line detectors. A low-amplitude background with a shape generated from event-mixing [30, 31] is consistent with a high-statistics study performed with a similar experimental set-up [32]. Transitions strengths at 0.102(21), 0.546(58), and 2.92(12) MeV were identified in coincidence with the  $^{53}\text{Ca}$  ground state, at 0.1013(54), 0.583(13), 1.224(74), and 1.955(45) MeV with the 1738-keV state, and at 0.385(13), 0.672(21), and 1.454(33) MeV with the 2220-keV state. Summing the decay energies with their coincident  $^{53}\text{Ca}$  state energies suggests that the 2.92-, 1.224-, and 0.672-MeV decays depopulate a common state, as do the 1.955- and 1.454-MeV decays. The levels and their cross sections are summarized in Fig. 2(g). An exclusive PMD was extracted for the level strength at 6758 keV, as shown in Fig. 2(f), owing to its  $\sim 3$ -MeV decay being isolated in the  $E_{\text{rel}}$  spectrum of Fig. 2(b), and conforms to a  $d$ -wave proton removal. Other exclusive cross sections do not provide conclusive results. The inclusive PMD for the full  $E_{\text{rel}}$  strength, Fig. 2(e), is consistent with a  $d$ -wave proton removal. Assuming a  $\pi 0d_{3/2}$  proton removal and a  $7/2^-$   $^{55}\text{Sc}$  ground state, as suggested by Fig. 2(c), gives possible  $J^\pi = 2, 3, 4, 5^-$  for the unbound states. Therefore, most observed excited states shown in Fig. 2(g) are likely of  $\pi 0f_{7/2}^{-1} 0d_{3/2}^{-1}$  structure. The relative energy spectrum of  $^{55}\text{Sc}(p, 2p)^{54}\text{Ca}^* \rightarrow ^{52}\text{Ca} + 2n$  has too few statistics for

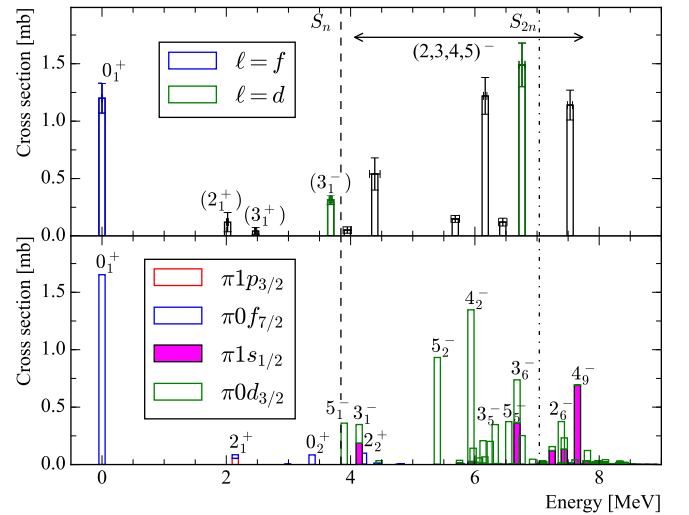


FIG. 3. (Top panel) Below  $S_n$ , the measured cross sections to states from  $\gamma$ -ray spectroscopy are shown. Above  $S_n$ , the population cross sections of the unbound states from invariant mass spectroscopy are shown at the energy centroids of fitted values and likely represent contributions from several states. States with conclusive PMDs are colored accordingly to the  $\ell$ -value of their removed nucleon, otherwise are black. (Bottom panel) Theoretical predictions of state energies and their population cross sections are shown. Contributions to cross sections from proton removals from the different orbitals are indicated. Unlabelled levels have  $J^\pi = 2, 3, 4, 5^-$ .

256 interpretation.

257 Figure 2(g) and the upper panel of Fig. 3 summarize measured level energies and population cross sections from this work. Theoretical cross sections and energies are displayed in the lower panel of Fig. 3. Energies were calculated from the conventional shell model using the GXPF1Br interaction in the full  $sd$ - $pf$ - $gds$  model space, including both  $0g_{7/2}$  and  $0g_{9/2}$  orbitals. Cross sections are those of the DWIA single-particle values scaled with spectroscopic factors from the same calculation as used for the energies [27]. Measured cross sections of the  $0_1^+$ ,  $2_1^+$  and  $(2_1^+)$ , 0.121(84) mb, states are reproduced by the calculated, 1.65 mb and 0.086 mb, respectively. Moreover, the measured  $(2_1^+)$  energy is in agreement with theory. Some population of the  $0_2^+$  state is predicted with a cross section consistent with that of the low-significance 561-keV  $\gamma$ -ray candidate, not shown on Fig. 3. To a very good approximation, the predicted  $3_1^+$  at 2.99 MeV has zero cross section, consistent with observation of the  $(3_1^+)$  state at the lower 2.47 MeV. The predicted  $3_1^-$  state is unbound, contrary to observation, however, the measured cross section, 0.316(43) mb, agrees well with the predicted 0.35 mb. It is noteworthy that similar contributions to the  $3_1^-$  state from the  $\pi 1s_{1/2}$ , 0.19 mb, and  $\pi 0d_{3/2}$ , 0.16 mb, orbitals are predicted. The state's experimental PMD shown in Fig. 2(d) does not reflect such a contribution. The inclusive cross

section to bound states was measured to be 1.69(3) mb, close to the predicted 1.83 mb, suggesting little quenching compared to what is expected from such reactions [33]. Above  $S_n$ , it is stressed that whilst the cross sections are indicated at the level energies shown in Fig. 2(g), they are likely distributed across many unresolvable states. Broadly speaking, the location of level strengths are in good agreement with prediction. Between  $S_n$  and  $S_{2n}$  a total level strength of 3.57(30) mb is observed, compared with predicted 5.30, 5.19, 4.87, and 4.75 mb considering the  $dfs$ ,  $ds$ ,  $df$ , and  $d$  contributions, respectively, and subtracting the  $3_1^-$  contribution. Beyond  $S_{2n}$ , within the experimentally sensitive range, 2.12, 2.09, 0.96, and 0.93 mb population strengths are predicted for  $dfs$ ,  $ds$ ,  $df$ , and  $d$  contributions, respectively, compared to a lower limit of  $>1.01$  mb deduced from a 1.14(13) mb strength in the  $1n$  channel. The over-prediction in the range  $S_n < E_{\text{level}} < S_{2n}$  may result from some levels predicted to lie below  $S_{2n}$  in-fact existing beyond it and decaying via  $2n$  emission, since the bound-state decays are well reproduced by the prediction, quenching of spectroscopic factors is unlikely. In addition, it is noted that exclusion of the deeply bound  $\pi 1s_{1/2}$  contribution lowers predicted cross section towards the measured value. As for cross sections of the strengths beyond  $S_{2n}$ , direct comparison to theory is difficult owing to the lack of sensitivity to the  $2n$  decay channel. If the bold assumption is made that the levels observed in the  $^{53}\text{Ca}+1n$   $E_{\text{rel}}$  spectra only decay via  $1n$  emission, excluding the  $\pi 1s_{1/2}$  contribution brings the predicted value to agreement with observation. Proton removal from  $\pi 0d_{3/2}$  dominates the excited states, reflected by the inclusive PMD. Whilst a strong population of the  $4_9^-$  state following  $\pi 1s_{1/2}$  proton removal is predicted it is not observed clearly in any PMD, possibly due to the influence of states populated by  $\pi 0d_{3/2}$  proton removal.

Negligible population of excited states of  $^{54}\text{Ca}$  originates from the proton removal from  $\pi 0f_{7/2}$  in  $^{55}\text{Sc}$ . All excited states are consistent with population from core-proton removals, predominantly from  $\pi 0d_{3/2}$ , and potentially  $\pi 1s_{1/2}$ . These findings are contrary to the analogous case of  $^{25}\text{F}(p, 2p)$  [13], in which valence proton removals preferentially populated excited states of  $^{24}\text{O}$ .

The shell model calculations result in  $0p-0h$  (closed  $N = 34$  shell) contributions of the  $^{55}\text{Sc}$  and  $^{54}\text{Ca}$  ground-state wavefunctions as 64.2% and 89.4%, respectively. The remainder of the contributions are dominated by  $2p-2h$  configurations. Despite this erosion of the  $N = 34$  closure in  $^{55}\text{Sc}$ , which is supported by experiment [34], the spectroscopic factors ( $C^2S$ ) show removal from  $\pi 0f_{7/2}$  mostly populates the ground-state of  $^{54}\text{Ca}$ , as observed experimentally. This can be understood through a simple two-level system of both  $^{55}\text{Sc}$  and  $^{54}\text{Ca}$ . Assuming each

$0h$  ( $\phi_{0p0h}$ ) and  $2p-2h$  ( $\phi_{2p2h}$ ) configurations,

$$\begin{aligned}\Psi(^{55}\text{Sc}) &= \alpha_{0p0h}\phi_{0p0h}(^{55}\text{Sc}) + \alpha_{2p2h}\phi_{2p2h}(^{55}\text{Sc}), \\ \Psi(^{54}\text{Ca}) &= \beta_{0p0h}\phi_{0p0h}(^{54}\text{Ca}) + \beta_{2p2h}\phi_{2p2h}(^{54}\text{Ca}),\end{aligned}$$

where  $\alpha$  and  $\beta$  are real numbers satisfying  $\alpha_{0p0h}^2 + \alpha_{2p2h}^2 = 1$  and  $\beta_{0p0h}^2 + \beta_{2p2h}^2 = 1$ . With vanishing overlaps of  $\phi_{0p0h}$  and  $\phi_{2p2h}$ , the spectroscopic factor to the ground state of  $^{54}\text{Ca}$  can be expressed as,

$$C^2S_{\text{g.s.}} = (\alpha_{0p0h}\beta_{0p0h} + \alpha_{2p2h}\beta_{2p2h})^2. \quad (1)$$

Since pairing forces have a definite sign in their off-diagonal two-body matrix elements, the amplitudes  $\alpha_{2p2h}$  and  $\beta_{2p2h}$  take on the same sign [14]. Therefore,  $\alpha_{2p2h}\beta_{2p2h} > 0$  leading to a large  $C^2S_{\text{g.s.}}$  following the removal of a valence proton. With  $\alpha_{0p0h} = 0.642$ ,  $\beta_{0p0h} = 0.894$ ,  $\alpha_{2p2h} = \sqrt{1 - \alpha_{0p0h}^2}$ , and  $\beta_{2p2h} = \sqrt{1 - \beta_{0p0h}^2}$ , Eq. 1 yields  $C^2S_{\text{g.s.}} = 0.907$ , and from the full calculation, including all other contributions,  $C^2S_{\text{g.s.}} = 0.828$  for the proton removal from  $\pi 0f_{7/2}$ . For the singly-occupied  $\pi 0f_{7/2}$  orbital,  $\sum C^2S \approx 1$ , leaving little remaining spectroscopic strength available to excited states. Therefore, despite the tensor-induced configuration mixing of the  $^{54}\text{Ca}$  core of  $^{55}\text{Sc}$ , conditions resulting from the pairing force lead to dominant ground-state population following valence proton removal.

In conclusion, the ground and excited states of the non-canonical doubly magic  $^{54}\text{Ca}$  have been populated through direct proton-knockout reactions on a  $\text{LH}_2$  target from  $^{55}\text{Sc}$ . Orbital angular momenta of removed protons were inferred through PMDs of reaction residues. The level scheme of  $^{54}\text{Ca}$  [7] was expanded to beyond the  $S_{2n}$  threshold through  $\gamma$ -ray and invariant-mass spectroscopy. The latter being for the first time applied to such a heavy neutron-rich system. All observed excited states populated through the  $^{55}\text{Sc}(p, 2p)$  reaction were attributed to removal of protons from the  $^{54}\text{Ca}$  core. Valence-proton removals populated predominantly the ground-state of  $^{54}\text{Ca}$  despite significant neutron-excitation amplitudes in the ground-state configuration of  $^{55}\text{Sc}$ . The reasoning behind this was the constructive effects from the pairing interaction on the ground state spectroscopic factor, exhausting the strength available to excited states. Considering the ubiquity of the pairing interaction, it is interesting this effect is seemingly overridden by tensor forces in the  $^{25}\text{F}(p, 2p)$  case [13]. It is noteworthy that the experiment carried out in Ref. [13] did not have beam-velocity neutron-detection capability. An experiment similar to the one reported here would enable the population of individual unbound states of  $^{24}\text{O}$  to be quantitatively studied, leading to a more robust comparison to the predicted spectroscopic factors. With such information, the interplay of the tensor and pairing interactions in direct reactions could be consolidated.

Our gratitude is extended to the RIKEN Nishina Cen-

386 ter accelerator staff for the stable and high-intensity  
 387 transport of the Zn primary beam, and the BigRIPS team  
 388 for their preparation of the magnetic settings of the sec-  
 389 ondary beam. F. B. is supported by the RIKEN Special  
 390 Postdoctoral Researcher Program. S. C. acknowledges  
 391 support from the IPA program at the RIKEN Nishina  
 392 Center. K. O. and K. Y. acknowledge the support from  
 393 Grants-in-Aid of the Japan Society for the Promotion of  
 394 Science under Grants No. JP16K05352. This work was  
 395 supported by JSPS KAKENHI Grants No. JP16H02179  
 396 and JP18H05404, the DFG under Grant No. BL 1513/1-  
 397 1 HGS-HIRe, the BMBF (grant No. 05P19RDFN1),  
 398 Swedish Research Council under Grant Nos. 621-2014-  
 399 5558 and 2019-04880. L.X.C and B.D.L are supported by  
 400 the Vietnam MOST via the Physics Development Pro-  
 401 gram Grant No. ĐTĐLCN.25/18. D. So. was supported  
 402 by the the European Regional Development Fund con-  
 403 tract No. GINOP-2.3.3-15-2016-00034 and the National  
 404 Research, Development and Innovation Fund of Hungary  
 405 via Project No. K128947.

(2014).

- 443 [22] I. Murray *et al.*, RIKEN Accel. Prog. Rep. **51**, 158 (2018).  
 444 [23] T. Kobayashi *et al.*, *Nucl. Instrum. Methods Phys. Res.,*  
 445 *Sect. B* **317**, 294 (2013).  
 446 [24] C. Santamaria *et al.*, *Nucl. Instrum. Methods Phys. Res.,*  
 447 *Sect. A* **905**, 138 (2018).  
 448 [25] T. Nakamura and Y. Kondo, *Nucl. Instrum. Methods*  
 449 *Phys. Res. Sect B* **376**, 156 (2016).  
 450 [26] T. Aumann, *Technical Report for the design, construction*  
 451 *and commissioning of NeuLAND: The high-resolution*  
 452 *neutron time-of-flight spectrometer for R3B*, Tech. Rep.  
 453 (FAIR, 2011).  
 454 [27] See Supplemental Material at [URL will be inserted by  
 455 publisher] for inclusive and ( $2_1^+$ ) PMDs, exclusive  $E_{\text{rel}}$   
 456 spectra and associated fit details, full results of theoretical  
 457 calculations.  
 458 [28] H. L. Crawford *et al.*, *Phys. Rev. C* **82**, 014311 (2010).  
 459 [29] A. M. Lane and R. G. Thomas, *Rev. Mod. Phys.* **30**, 257  
 460 (1958).  
 461 [30] G. Randisi *et al.*, *Phys. Rev. C* **89**, 034320 (2014).  
 462 [31] S. Leblond *et al.*, *Phys. Rev. Lett.* **121**, 262502 (2018).  
 463 [32] A. Revel *et al.* (SAMURAI21 collaboration), *Phys. Rev.*  
 464 *Lett.* **124**, 152502 (2020).  
 465 [33] J. A. Tostevin and A. Gade, *Phys. Rev. C* **90**, 057602  
 466 (2014).  
 467 [34] D. Steppenbeck *et al.*, *Phys. Rev. C* **96**, 064310 (2017).

\* frank@ribf.riken.jp

† Present address: Instituto de Estructura de la Materia,  
 CSIC, E-28006 Madrid, Spain

- 406 [1] N. Paul *et al.*, *Phys. Rev. Lett.* **122**, 162503 (2019).  
 407 [2] M. G. Mayer, *Phys. Rev.* **75**, 1969 (1949).  
 408 [3] O. Haxel, J. H. D. Jensen, and H. E. Suess, *Phys. Rev.*  
 409 **75**, 1766 (1949).  
 410 [4] T. Otsuka, T. Suzuki, R. Fujimoto, H. Grawe, and  
 411 Y. Akaishi, *Phys. Rev. Lett.* **95**, 232502 (2005).  
 412 [5] T. Otsuka, R. Fujimoto, Y. Utsuno, B. A. Brown,  
 413 M. Honma, and T. Mizusaki, *Phys. Rev. Lett.* **87**, 082502  
 414 (2001).  
 415 [6] T. Otsuka, A. Gade, O. Sorlin, T. Suzuki, and Y. Ut-  
 416 suno, *Rev. Mod. Phys.* **92**, 015002 (2020).  
 417 [7] D. Steppenbeck *et al.*, *Nature (London)* **502**, 207 (2013).  
 418 [8] S. Michimasa *et al.*, *Phys. Rev. Lett.* **121**, 022506 (2018).  
 419 [9] S. Chen *et al.*, *Phys. Rev. Lett.* **123**, 142501 (2019).  
 420 [10] A. Obertelli *et al.*, *Phys. Lett. B* **633**, 33 (2006).  
 421 [11] C. R. Hoffman *et al.*, *Phys. Rev. Lett.* **100**, 152502  
 422 (2008).  
 423 [12] R. Kanungo *et al.*, *Phys. Rev. Lett.* **102**, 152501 (2009).  
 424 [13] T. L. Tang *et al.*, *Phys. Rev. Lett.* **124**, 212502 (2020).  
 425 [14] S. Yoshida, *Nucl. Phys.* **33**, 685 (1962).  
 426 [15] K. Ogata, K. Yoshida, and K. Minomo, *Phys. Rev. C*  
 427 **92**, 034616 (2015).  
 428 [16] T. Wakasa, K. Ogata, and T. Noro, *Prog. Part. Nucl.*  
 429 *Phys.* **96**, 32 (2017).  
 430 [17] F. Wienholtz *et al.*, *Nature (London)* **498**, 346 (2013).  
 431 [18] T. Kubo *et al.*, *Prog. Theor. Exp. Phys.* **2012**, 03C003  
 432 (2012).  
 433 [19] N. Fukuda, T. Kubo, T. Ohnishi, N. Inabe, H. Takeda,  
 434 D. Kameda, and H. Suzuki, *Nucl. Instrum. Methods*  
 435 *Phys. Res., Sect. B* **317**, 323 (2013).  
 436 [20] A. Obertelli *et al.*, *Eur. Phys. J. A* **50**, 8 (2014).  
 437 [21] S. Takeuchi, T. Motobayashi, Y. Togano, M. Matsushita,  
 438 N. Aoi, K. Demichi, H. Hasegawa, and H. Murakami,  
 439 *Nucl. Instrum. Methods Phys. Res., Sect. A* **763**, 596  
 440 (2014).